Bull. Mater. Sci., Vol. 37, No. 6, October 2014, pp. 1403–1409. © Indian Academy of Sciences.

Conductivity study of PEO–$LiClO_4$ polymer electrolyte doped with ZnO nanocomposite ceramic filler

S U PATIL[a,*], S S YAWALE[b] and S P YAWALE[c]

[a]Department of Applied Physics, Govt. College of Engineering, Chandrapur 442 403, India
[b]Pre-Indian Administrative Services Training Institute, Nagpur 440 001, India
[c]Department of Physics, Govt. Vidarbha Institute of Science and Humanities, Amravati 444 604, India

MS received 20 February 2013; revised 10 October 2013

Abstract. The preparation and characterization of composite polymer electrolytes comprising PEO and $LiClO_4$ with different concentrations of ZnO nanoparticles are studied. Conductivity measurements were carried out and discussed. In order to ascertain the thermal stability of the polymer electrolyte with maximum conductivity, films were subjected to TG/DTA analysis in the range of 298–823 K. In the present work, FTIR spectroscopy is used to study polymer structure and interactions between PEO and $LiClO_4$, which can make changes in the vibrational modes of the atoms or molecules in the material. FTIR spectra show the complexation of $LiClO_4$ with PEO. The SEM photographs indicated that electrolytes are miscible and homogeneous.

Keywords. Composite electrolyte; ceramic filler; poly(ethylene oxide); ZnO; ionic conductivity; impedance spectroscopy.

1. Introduction

The properties of polymer electrolytes such as their high compliance, good adherence to electrodes and the possibility of fabricating the polymers into thin films are attractive for advanced applications such as high-energy density rechargeable batteries (MacCallum and Vincent 1987; Gray 1997), chemical sensors, electrochemical capacitors, analog memory devices and many more. An exemplary solid polymer electrolyte is a poly(ethylene oxide) (PEO) system containing lithium salts (Ahn *et al* 2003; Kwang-Sun Ji *et al* 2003; Shin and Passerini 2004; Suarez *et al* 2004). In the case of PEO : LiX electrolytes, the ions are transported by the semi-random motion of short polymer segments. The segmental motions promote ion mobility by making and breaking coordination bonds between cation and polymer. This provides free volume into which the ion can diffuse under the influence of an electric field. Cations moving between coordinating sites adopt transient state where cations are coordinated by both anions and polymer chain sites, before the segmental motion of polymer breaks one coordinating bond (Kumar and Lawrence 2000). However, polymer in such a system tends to crystallize, resulting in a low room temperature ionic conductivity unsuitable for practical application. Two approaches have been developed to solve this problem, that is, incorporation of plasticizers (Yang *et al* 1995; Michael *et al* 1997; Reddy *et al* 1999; Kim and Smotkin 2002) and ceramic fillers. The major issues in these modifications are focused on improving ionic conductivity, mechanical properties and interfacial stability with lithium electrode (Przluski *et al* 1990; Kumar and Scanlon 1994; Croce *et al* 1995; Zhaohui Li *et al* 2003). Also, large surface area of the solid oxide filler prevents locking in high degree of disorder and favours high ion transport. Various studies have interpreted the role of filler in terms of Lewis acid–base model interaction (Wieczorek *et al* 1996; Chung *et al* 2001; Croce *et al* 2001). According to this model, oxide ceramic fillers dispersed in PEO–LiX electrolyte form complexes with the basic oxygen atoms in the PEO chains and act as cross-linking centres for PEO segments, and thereby reduce polymer chain reorganization and promote Li^+ transport at the boundaries of the filler particles (Croce *et al* 1999).

An extensive literature survey (Capiglia *et al* 1999; Walls *et al* 2000; Chu and Reddy 2003) shows that almost all polymer ceramic nanocomposites were prepared through mechanical blending of nanoscale ceramic particles, polymer and salt in a compatible solvent. Few studies have been published using sol–gel process, in which nanosize ceramic fillers are precipitated in the polymer matrix (Ahn *et al* 2003; Liu *et al* 2004). However, in sol–gel process, precursors may not be completely converted into nanosize ceramic fillers after hydrolysis and condensation reactions. In this study, solid polymer electrolytes was prepared by the addition of nanosized ZnO particles to PEO–$LiClO_4$. The range of ZnO concentration is

*Author for correspondence (s19_patil@yahoo.co.in; shishirupatil@gmail.com)

kept narrow to find precise high conductivity concentration. In our study, we have used inorganic molecule filler (ZnO) because organic molecule fillers are more expensive compared to inorganic molecule filler. Ionic conductivity and morphology of the composite polymer electrolytes films were examined by d.c., a.c. impedance spectroscopies and SEM. Electrolytes are also characterized by TG/DTA and FTIR measurements. Our results show that change in the concentration of ZnO nanoparticles in the PEO–$LiClO_4$ matrix changes the mechanical stabilities and the ionic conductivity of the composite polymer electrolytes.

2. Experimental

2.1 *Materials*

Poly(ethylene oxide) (PEO) (MW: 300000) was obtained from Alfa Aesar, Ward Hill, MA 01835, USA. Zinc oxide (ZnO) nanopowder (Purity: 99%, APS: 20 nm) was purchased from Nanoshell, Wilmington, DE 19808, USA. Lithium perchlorate ($LiClO_4$) was analytically pure and dried at 353 K for one day before use. Acetonitrile was used as the solvent in the film casting process.

2.2 *Preparation of composite polymer electrolyte films*

Poly(ethylene oxide) (PEO)/$LiClO_4$ weight ratio was fixed at 90 : 10 and the mixture was blended with various weight percentages of ZnO nanopowder. To prepare composite samples, first, a predetermined amount of $LiClO_4$ and *m*-ZnO nanopowder were dissolved in acetonitrile. The solution was stirred for 1 h and, then, a calculated amount of PEO was added to the solution. The mixture was stirred vigorously for 5–6 h to obtain a homogeneous mixture. Films were obtained by transferring the mixture on the plane teflon plate. Films were first dried in the open atmosphere to allow the solvents to evaporate and then dried in vacuum for 24 h to completely remove the residual traces.

2.3 *Impedance measurement*

Surface morphology was studied by means of JSM–7600F field emission fun–scanning electron microscope at SAIF, Indian Institute of Technology, Mumbai. The thermal stability of the electrolytes was characterized by TG/DTA technique. The IR spectra were recorded on Shimadzu IR Affinity-I FTIR spectrophotometer in the range of 4000–400 cm^{-1}. A.C. impedance of the composite electrolyte films was measured by using Wayne Kerr 4230 LCR meter (UK) between 100 Hz and 200 kHz with 0·5 V amplitude. The films were sandwiched between two copper electrodes in a sample holder.

3. Results and discussion

3.1 *Scanning electron microscopy (SEM) analysis*

Figure 1 shows the surface morphology of optimized samples of the PEO–$LiClO_4$–*m*ZnO electrolytes. The samples are completely amorphous and homogeneous. No crystals were developed in the samples containing 9 and 10 wt% of ZnO. Figure 1(a, b) shows the smooth surface morphology. Smooth morphology is related to the reduction of PEO crystalline with lithium salt. As the concentration of ZnO nanoparticles increases, streak development increases on the smooth surface and severe phase-separated domains also increases with the concentration of ZnO nanoparticles (figure 1(b, c)). Changes in the texture and morphology of electrolytes indicate the slight interaction of ZnO nanoparticles with the polymer system.

3.2 *Thermal analysis (TG/DTA)*

Thermal stability of a polymer electrolyte is also an important parameter to guarantee acceptable performances in lithium batteries. In order to ascertain the thermal stability films of optimized samples having highest conductivity are subjected to TG/DTA analysis in the range of 298–823 K at a heating rate of 10 K/min. Figure 2 shows that for 9, 10 and 11 wt% ZnO-doped films melting temperature (T_m) is at 337·92, 339·46, 338·52 K, respectively, which shows that glass transition temperature (T_g) of these films is low, i.e. below 273 K. For 9, 10 and 11 wt% ZnO-doped films TG curve shows first degradation at 351, 373 and 358 K accompanied by a weight loss of 5, 3·4 and 5·5%, respectively. This degradation may be due to the evaporation of moisture absorbed by the sample during loading (Scott and Macosko 1995). This first step of degradation is asserted by the DTA curve giving an endothermic peak at 337·92, 339·46 and 338·52 K for 9, 10 and 11 wt% ZnO-doped composite electrolytes, respectively. The composite electrolytes are found to be stable up to 471, 475 and 469 K for 9, 10 and 11 wt% ZnO, respectively, with a weight loss of 1%. Rapid weight loss observed in the TG curve after 471, 475 and 469 K indicates the complete decomposition of composite electrolyte, which is evidenced by the exothermic peaks observed in the DTA curves for 9, 10 and 11 wt% ZnO, respectively.

3.3 *Fourier transform infrared spectra*

The FTIR spectra are obtained in the range of 4000–400 cm^{-1} at room temperature (figure 3). Only three samples are selected, including optimized sample. The peaks are sharp and broad. In all, 18–20 peaks are observed. The bands are appeared around 3200–3600 cm^{-1} assigned for O–H group and intermolecular hydrogen

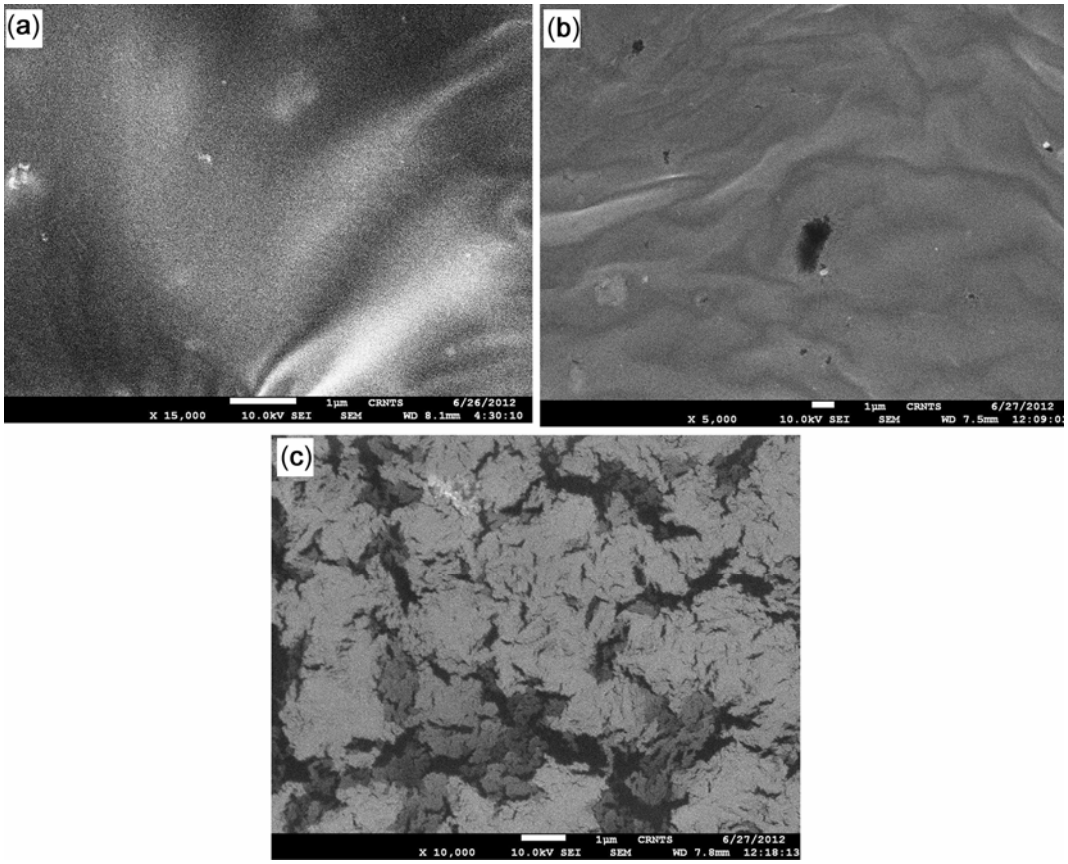

Figure 1. SEM photographs of PEO–$LiClO_4$–*m*ZnO electrolyte: (**a**) m = 9 wt%, (**b**) m = 10 wt% and (**c**) m = 11 wt%.

bonding. It was observed that the samples are hygroscopic in nature, hence they absorb moisture from the environment easily.

The width of absorption band appearing between 2950 and 2800 cm^{-1} was found to increase with an increase in doping concentration and the band shifts towards the lower frequency region. The vibrational frequencies, 1450 and 820 cm^{-1}, are assigned to CH_2 scissoring and wagging mode of pure PEO. The absorption peaks corresponding to scissoring mode of PEO appearing at 1450 cm^{-1} in pure PEO is shifted to 1448·5, 1463·93 and 1479·36 cm^{-1} for 9, 10 and 11 wt% ZnO doping. The vibrational frequency, 820 cm^{-1}, is shifted to 846·73 cm^{-1}. In addition to this, CH_2 waging mode at around 1360 cm^{-1} in pure PEO is shifted to lower frequency region with increase in doping concentration. This decrease in wavenumber results in increase in bond length and, hence, complexation takes place. The vibrational frequency corresponding to CH_2 rocking mode is appearing at 939·31, 954·74 and 939·31 cm^{-1} for 9, 10 and 11 wt% ZnO doping. CH asymmetrical stretching frequency of 1950 cm^{-1} in pure PEO is shifted to 1957·69 cm^{-1} in the complexes. The band appearing between 1030 and 1160 cm^{-1} corresponds to C–O–C symmetric and asymmetric stretching. The vibrational frequency of 626 cm^{-1} corresponding to $LiClO_4$ is shifted to 630·71 cm^{-1} in the complexes. Absorption peaks in the range of 400–500 cm^{-1} are attributed to stretching vibrations of ZnO. The vibrational frequency of 1649·09 cm^{-1} corresponding to OH bond belongs to water molecule. Some new peaks are present in the spectra. The appearance of new peaks along with changes in the existing peaks and/or their disappearance in the IR spectra directly indicates the complexation of $LiClO_4$ with PEO (Papke *et al* 1981, 1982; Mitra and Kulkarni 2002; Sharma and Sekhon 2005; Mohan *et al* 2007; Noor *et al* 2010).

3.4 *Conductivity studies of composite electrolyte film*

Figure 4 shows the a.c. impedance spectra of PEO–$LiClO_4$–*m* wt% ZnO composite electrolyte films and equivalent circuit of the electrochemical cell for impedance measurement, where R_1 is resistance of cell besides electrolyte film. R_b and C_b are resistance and capacitance of electrolyte film, respectively. C_e is electrode–electrolyte interfacial capacitance. The point of insertion between the arc in the high-frequency range and the straight line in the low-frequency range coincides with the bulk

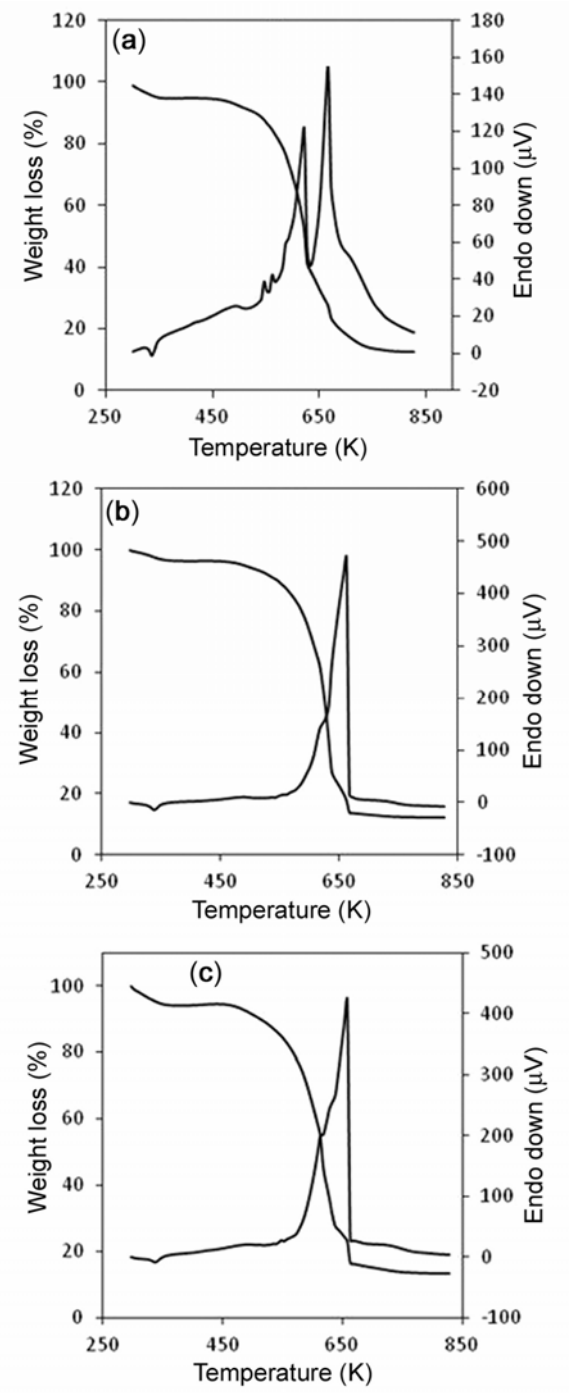

Figure 2. TG/DTA plots for PEO–$LiClO_4$–*m*ZnO electrolyte: (**a**) *m* = 9 wt%, (**b**) *m* = 10 wt% and (**c**) *m* = 11 wt%.

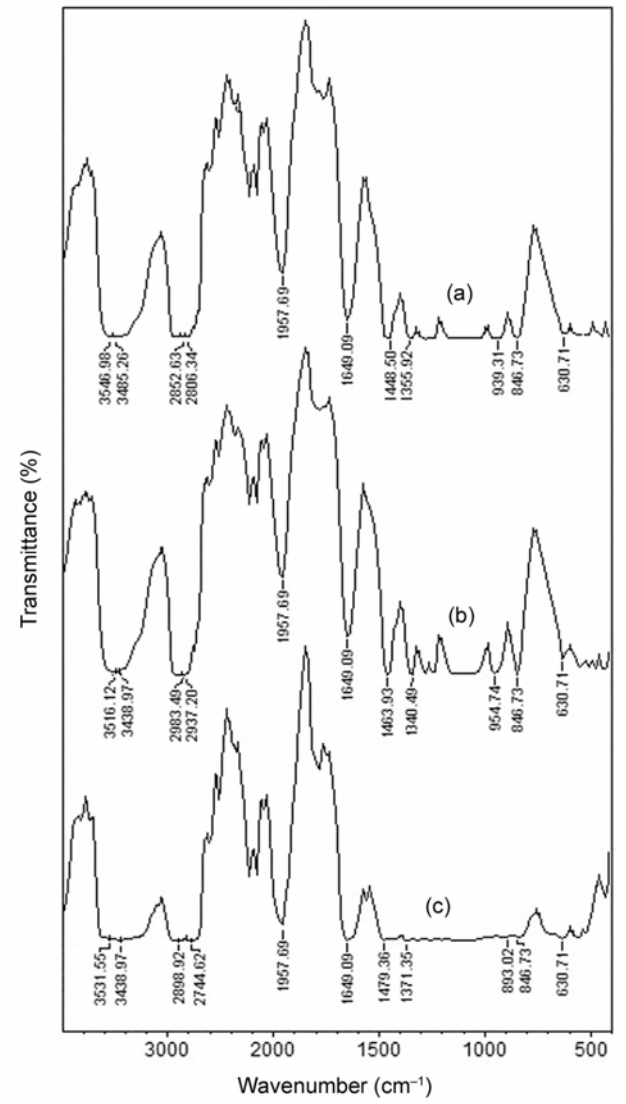

Figure 3. FTIR spectra of PEO–$LiClO_4$–*m*ZnO electrolyte: (a) *m* = 9 wt%, (b) *m* = 10 wt% and (c) *m* = 11 wt%.

resistance of composite electrolyte films. In our experiment, the complete semicircles in the high-frequency range are not observed, which may be concluded that the frequency is not high enough. The high-frequency semicircle corresponds to the bulk response of the films. The curves at the low temperature suggest that the migration of ions occur through the volume of matrix polymer, which can be represented by a resistor. The immobile polymer chains, on the other hand, become polarized in the alternating field, and can therefore be represented by a capacitor. The ionic migration and bulk polarization are physically in parallel, and therefore, the portion of the semicircle can be observed at high frequencies (Reddy *et al* 2006).

From figure 4, we can predict that the magnitude of the high-frequency semicircle decreases as a result of its shift to higher frequency due to an increase in ionic conductivity. We can directly read the bulk resistance of the electrolyte (R_b) from the intercept of the impedance spectrum on the Z' real axis. The ionic conductivity of the polymer electrolyte can then be calculated from the relation

$$\sigma = t/(R_b A), \tag{1}$$

where t is the thickness of the electrolyte film, A the area of the electrolyte film and R_b the bulk resistance of the electrolyte film. The ionic conductivities measured by

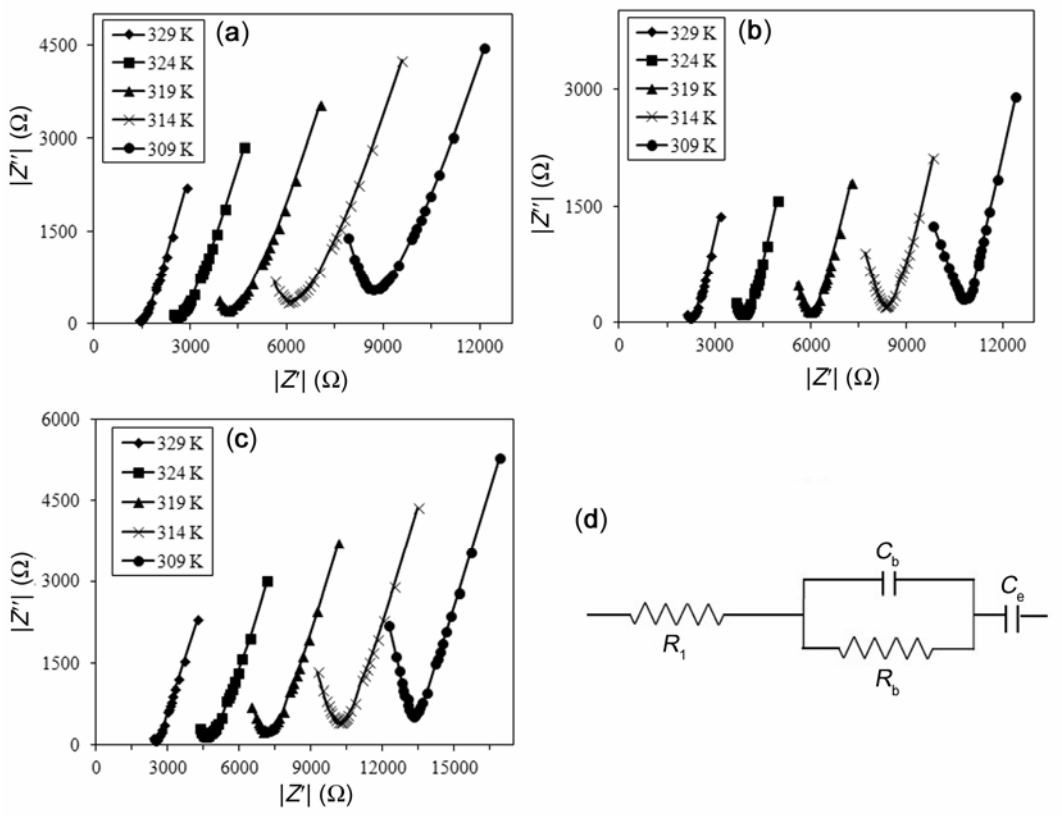

Figure 4. A.C. impedance spectra of composite electrolyte films: (**a**) PEO–LiClO$_4$–9% ZnO, (**b**) PEO–LiClO$_4$–10% ZnO, (**c**) PEO–LiClO$_4$–11% ZnO and (**d**) equivalent circuit for impedance measurement.

Table 1. Conductivity, activation energy and tranference of PEO–LiClO$_4$–*m*ZnO electrolyte.

Polymer electrolyte	Bulk resistance (R_b) at 309 K (Ω)	Grain boundary resistance (R_{gb}) at 309 K (Ω)	Ionic conductivity at 309 K (S/cm^2)	Activation energy (eV)	Transference number	
					t_{ion}	t_{ele}
PEO–LiClO$_4$–9% ZnO	9·077	8·805	$1{\cdot}20 \times 10^{-5}$	0·39	0·89	0·11
PEO–LiClO$_4$–10% ZnO	10·949	10·800	$1{\cdot}28 \times 10^{-5}$	0·41	0·88	0·12
PEO–LiClO$_4$–11% ZnO	13·371	13·175	$1{\cdot}21 \times 10^{-5}$	0·33	0·85	0·15

a.c. impedance spectroscopy at room temperature 309 K are presented in table 1. The data show that maximum conductivity for 10 wt% ZnO added films. The increase in conductivity is due to the formation of charge transfer complexes or decreases in the crystallization of electrolyte (Reddy *et al* 2006), while the decrease in conductivity for higher concentration is due to formation of ionic aggregates, which impede the conduction process and decrease the conductivity.

Figure 5(a) shows the temperature dependency of the d.c. conductivity for composite polymer electrolyte films. The plot of $\log \sigma$ vs $1000/T$ is approximately linear, suggesting the Arrhenius equation could be a good fit for the experimental data

$$\sigma = \sigma_0 \exp[-E_a/kT], \quad (2)$$

where σ_0 is the pre-exponential factor, E_a the activation energy and k is Boltzmann constant.

Activation energies for ion conductivity calculated from the Arrhenius relationships are summarized in table 1. Activation energy initially increases and then decreases with increase in the concentration of ZnO nanoparticles. It is also generally believed that there are interactions among ZnO, Li salt and polymer chain (Chung *et al* 2001; Blaoise *et al* 2003; Johansoon and Jacobsson 2004). Addition of ZnO increases both the ion mobility and charge carrier concentration which enhances the conductivity of composite electrolyte.

Figure 5(b) shows that the d.c. conductivity increases with increasing the ZnO content and attains a maximum value when the mass fraction of ZnO is 10%. Subsequently, the conductivity decreases with further increase

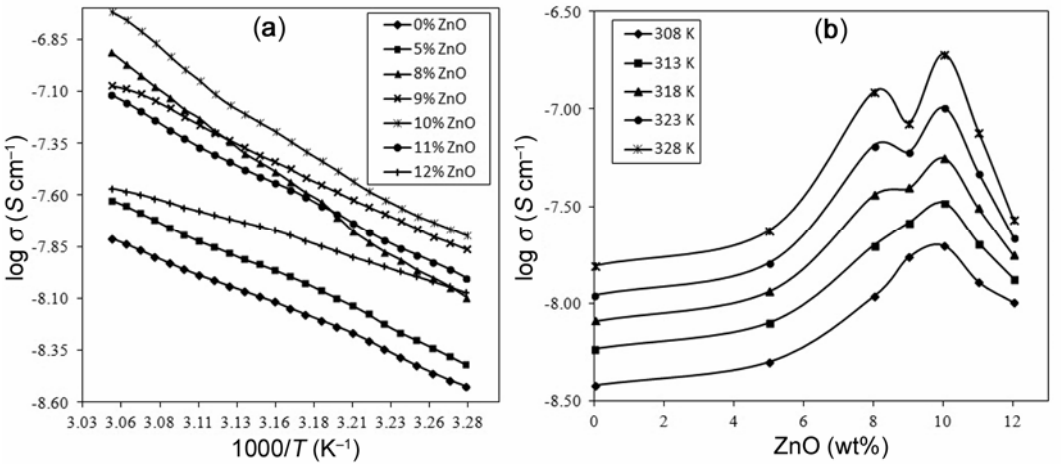

Figure 5. (**a**) Temperature-dependent d.c. conductivity for PEO–$LiClO_4$–*m*ZnO electrolyte, (**b**) variation of d.c. conductivity with ZnO (wt%) for PEO–$LiClO_4$–*m*ZnO electrolyte at different temperature.

in the ZnO content. The conductivity decreases due to bad dispersion of ZnO particles, resulting in the blocking of conduction paths. With increase in concentration of ZnO nanoparticles due to increase in phase-separated domains, texture of polymer network changes so drastically that the polymer fully covers the ZnO filler particles and blocking effect increases.

The transference number of an ion is the fraction of the total current that is carried by the respective ion across a given medium. Lithium ion transference number is calculated for optimized samples by applying a constant potential bias to a copper/electrolyte/lithium cell. Lithium ion transference number is calculated by using the equation

$$t_{ion} = I_s/I_o,$$

where I_s is the final steady-state current and I_o the initial current. The value of t_{ion} for the optimized samples listed in table 1 indicates that the charge conduction is predominantly ionic.

4. Conclusions

Nanocomposite polymer electrolytes comprising PEO and $LiClO_4$ with different concentrations of ZnO nanopowder are synthesized. SEM images show that polymer and ceramic fillers are uniformly mixed and the surface morphology is smooth up to 10 wt% ZnO concentration. When the ZnO wt% increase above 10 wt%, the phase-separated domain increases. Good thermal stability of polymer electrolyte systems up to 471, 475 and 469 K, for 9, 10 and 11 wt% ZnO, respectively, was confirmed by TG/DTA analysis. FTIR study suggests the presence of some new peaks in pattern. The appearance of new peaks along with changes in the existing peaks and/or their disappearance in the IR spectra directly indicates the complexation of $LiClO_4$ with PEO. Electrochemical measurements show the improvement in the ionic conductivity and mechanical properties in the polymer electrolyte system. Conductivity shows the maximum value when the mass fraction of ZnO nanoparticles is 10 wt%. Ion conduction is found to be achieved by both random diffusion within the amorphous PEO and replacing the adjacent lithium vacancy on the doping surface. Since the polymer electrolyte exhibits good thermal stability and conductivity values, this can be used as an electrolyte in lithium batteries and other electrochemical devices.

References

Ahn J H, Wang G X, Liu H K and Dou S X 2003 *J. Power Sources* **422** 119

Blaoise A C, Donoso J P, Magon C J, Rosario A V and Pereira E C 2003 *Electrochem. Acta* **2239** 48

Capiglia C, Mustarelli P, Quartarone E, Tomasi C and Magistris A 1999 *Solid State Ionics* **73** 118

Chu P P and Reddy M J 2003 *J. Power Sources* **288** 115

Chung S H, Wang Y, Persi L, Croce F, Greenbaum S G, Scrosati B and Plichta E 2001 *J. Power Sources* **644** 97

Croce F, Appatechi G B, Persi L and Scrosati B 1995 *Nature* **557** 373

Croce F, Curini R, Martinelli A, Persi L, Ronci F, Scrosati B and Caminiti R 1999 *J. Phys. Chem.* **B103** 10632

Croce F, Persi L, Scrosati B, Serriano-Fiory F, Plichta E and Hendrickson A 2001 *Electrochim. Acta* **2457** 46

Gray F M 1997 *Polymer electrolytes* (Cambridge: Royal Society of Chemistry) Chap. 2

Johansoon P and Jacobsson P 2004 *Solid State Ionics* **73** 170

Kim Y T and Smotkin E S 2002 *Solid State Ionics* **29** 149

Kumar B and Scanlon L G 1994 *J. Power Sources* **261** 52

Kumar B and Lawrence G S 2000 *J. Electroceram.* **5** 127

Kwang-Sun Ji, Hee-Soo Moon, Jong-Wook Kim and Jong-Wan Park 2003 *J. Power Sources* **124** 117

Liu Y, Lee J Y and Hong L 2004 *J. Power Sources* **303** 129

MacCallum J R and Vincent C A 1987 *Polymer electrolyte reviews* (London: Applied Science) p. 285

Michael M S, Jacob M M E, Prabhaharam S R S and Radhakrishna S 1997 *Solid State Ionics* **167** 98

Mitra S and Kulkarni A R 2002 *Solid State Ionics* **37** 154

Mohan V M, Raja V, Balaji Bhargav P, Sharma A K and Narasimha Rao V V R 2007 *J. Polym. Res.* **283** 14

Noor S A M, Ahmed A, Talib I A and Raheman M Y A 2010 *Ionics* **161** 16

Papke B L, Ratner M A and Shriver D F 1981 *J. Phys. Chem. Solids* **493** 42

Papke B L, Ratner M A and Shriver D F 1982 *J. Electrochem. Soc.* **1434** 129

Przluski J, Such K, Wycilik H, Wieczorek W and Florjauc-Zyk Z 1990 *Synth. Met.* **241** 35

Reddy C V S, Sharma A K and Narasimha Rao V V R 2006 *Polymer* **1318** 47

Reddy C V S, Xia Han, Quan-Yao Zhu, Li-Qiang Mai and Wen Chen 2006 *Eur. Polym. J.* **3114** 42

Reddy M J, Sreekanth T and Subba Rao U V 1999 *Solid State Ionics* **55** 126

Scott C E and Macosko C W 1995 *Polymer* **461** 36

Sharma J L and Sekhon S S 2005 *Ind. J. Eng. Mater. Sci*, **557** 12

Shin J H and Passerini S 2004 *Electrochem. Acta* **1605** 49

Suarez S, Abbrent S, Greenbaum S G, Shin J H and Passerini S 2004 *Solid State Ionics* **407** 166

Walls H J, Zhou J, Yerian J A, Fedkiw P S, Khan S A, Stowe M K and Baker G L 2000 *J. Power Sources* **156** 89

Wieczorek W, Stevens J R and Florjanczyk Z 1996 *Solid State Ionics* **67** 85

Yang X Q, Lee H S, Hanson L, McBreen J and Okamoto Y 1995 *J. Power Sources* **198** 54

Zhaohui Li, Guangyao Su, Xiayu Wang and Deshu Gao 2003 *Chem. J. Chin. Univ.* **2065** 11